NUMERICAL STUDY OF PARTICLE DIAMETER EFFECT ON OSCILLATORY SHEET FLOW TRANSPORT WITH MOVABLE BED SIMULATOR

Abbas YEGANEH-BAKHTIARY [1], Hitoshi GOTOH [2] and Tetsuo SAKAI [3]

[1] Member of JSCE, Dr. of Eng., JSPS postdoctoral fellow, Graduate School of Civil Eng., Kyoto Univ. (Yoshida Hon-machi, Sakyo-ku, Kyoto 606-8501, Japan).
[2] Member of JSCE, Dr. of Eng., Assoc. Prof., Graduate School of Civil Eng., Kyoto Univ. (ditto).
[3] Fellow of JSCE, Dr. of Eng., Professor, Graduate School of Civil Eng., Kyoto Univ. (ditto).

Numerical simulation of the sediment transport based on the Lagrangian method is one of the most viable methods to investigate the complex mechanism of oscillatory sheet flow. Not only the flow unsteadiness with containing sediment particles, which respond to the flow acceleration and deceleration process, but also the interparticle collision of the moving particles complicate the simulation task. In this study, the sediment motion is simulated with the aid of the Movable Bed Simulator code based on DEM model in which the frequent collision of the moving particles is sophisticatedly modeled. And the particle diameter effect on the developing time-dependent process of sheet flow transport is investigated, using three different diameter sizes of sediment. The different tendency in sheet flow transport can be explained as a relaxation process related to the time lag of flow velocity and the sediment motion, which responds to the flow acceleration and deceleration. Also, the time lag of the sediment motion in the sheet flow layer is evidently influenced by the particle diameter size.

Key Words: *Sheet flow, Movable Bed Simulator (MBS), DEM, Oscillatory flow.*

1. INTRODUCTION

Severe beach topography change often takes place during stormy wave condition when sheet flow mode of sediment transport is predominant. Sheet flow mode of transport is conventionally refereed to the bed-load transport at high shear stress where the transport occurs in a layer very close to the bed with a thickness of several times of the particle diameter. The difficulties in measuring of this phenomenon in the natural beach condition motivate researchers to reproduce it in the laboratory with oscillatory wave tunnels.

Experimental studies indicate that the physical property of particle affects the dynamics of sheet flow, but how and under which mechanism is not clearly verified. For example, Yeganeh and Asano[1)] have discussed on the systematic effects of particle properties on the dynamics of oscillatory sheet flow. They argued that the dispersive stress generated by interparticle collision depends mainly on the particle diameter, and the larger particle is, the less quickly particle responds to the flow acceleration and deceleration.

On the other hand, the complexity of the physics involved in the dynamics of sheet flow implies the applicability of numerical simulation as the most viable techniques to understand the hydrodynamics of transport. Gotoh and Sakai[2)] performed a pioneer work on the simulation of the sheet flow transport from the viewpoint of granular material dynamics. In their model the sediment motion as well as the frequent interparticle collision of the moving particles is simulated with using a Lagrangian method, based on the *Distinct Element Method*, which is an explicit numerical method and originally proposed by Cundall and Strack[3)].

The objective of the present numerical study is to investigate the developing mechanism of the sheet flow transport with a two-phase flow model in which the sediment particle response to the flow acceleration and deceleration process is traced from the Lagranigian point of view. Furthermore, the particle diameter effect on the developing time-dependent process of sheet flow transport is also studied by using three different diameter sizes of sediment. The flow phase in the model is described by the oscillatory flow; whereas, the sediment motion is simulated with the aid of *Movable Bed Simulator* (MBS) code based on the DEM model of Gotoh and Sakai[2)], in which the frequent collision of the moving particles is directly simulated.

2. HYDRODYNAMIC MODEL

(1) Model of fluid phase

The governing equations of the fluid phase is described with a vertically two-dimensional k-ε turbulence model as follows:

$$\frac{\partial U}{\partial x}+\frac{\partial V}{\partial y}=0 \tag{1}$$

$$\frac{\partial U}{\partial t}+U\frac{\partial U}{\partial x}+V\frac{\partial U}{\partial y}=-\frac{1}{\rho}\frac{\partial P}{\partial x}+\frac{\partial}{\partial x}\left(2\Gamma\frac{\partial U}{\partial x}\right)+\frac{\partial}{\partial y}\left[\Gamma\left(\frac{\partial U}{\partial y}+\frac{\partial V}{\partial x}\right)\right] \tag{2}$$

$$\frac{\partial V}{\partial t}+\frac{\partial V}{\partial x}+V\frac{\partial V}{\partial y}=-\frac{1}{\rho}\frac{\partial P}{\partial y}+\frac{\partial}{\partial x}\left[\Gamma\left(\frac{\partial U}{\partial y}+\frac{\partial V}{\partial x}\right)\right]+\frac{\partial}{\partial y}\left(2\Gamma\frac{\partial V}{\partial y}\right) \tag{3}$$

$$\frac{\partial k}{\partial t}+U\frac{\partial k}{\partial x}+V\frac{\partial k}{\partial y}=\frac{\partial}{\partial x}\left[\left(\nu+\frac{\nu_t}{\sigma_k}\right)\frac{\partial k}{\partial x}\right]+\frac{\partial}{\partial y}\left[\left(\nu+\frac{\nu_t}{\sigma_k}\right)\frac{\partial k}{\partial y}\right]+P_r-\varepsilon \tag{4}$$

$$\frac{\partial \varepsilon}{\partial t}+U\frac{\partial \varepsilon}{\partial x}+V\frac{\partial \varepsilon}{\partial y}=\frac{\partial}{\partial x}\left[\left(\nu+\frac{\nu_t}{\sigma_\varepsilon}\right)\frac{\partial \varepsilon}{\partial x}\right]+\frac{\partial}{\partial y}\left[\left(\nu+\frac{\nu_t}{\sigma_\varepsilon}\right)\frac{\partial \varepsilon}{\partial y}\right]+\frac{\varepsilon}{k}\left(C_{1\varepsilon}P_r-C_{2\varepsilon}\varepsilon\right) \tag{5}$$

$$P_r=2\nu_t\left[\left(\frac{\partial U}{\partial x}\right)^2+\left(\frac{\partial V}{\partial y}\right)^2+\left(\frac{\partial U}{\partial x}+\frac{\partial V}{\partial y}\right)^2\right] \tag{6}$$

$$\Gamma=\nu+\nu_t \quad ; \quad \nu_t=C_\mu\frac{k^2}{\varepsilon} \tag{7}$$

in which U, V=mean flow velocity in x, y direction; x, y=streamwise and upward-vertical coordinates; ρ=mass density of water; P=pressure; Γ=effective viscosity; k=turbulent kinetic energy; ν=kinematic viscosity; ν_t=kinematic eddy viscosity; P_r=production of turbulent kinetic energy due to shear stress; and ε=dissipation of turbulent kinetic energy. The constants in k-ε model are as follows: C_μ=0.09; σ_k=1.0; σ_ε=1.3; $C_{1\varepsilon}$= 1.44; and $C_{2\varepsilon}$=1.92.

(2) Sediment phase model

The sediment particles are modeled by spherical particles with uniform diameters, and their motions are numerically traced in a vertically two-dimensional plane. Among each particle, spring-dashpot system is introduced to express the particle/particle interaction. The equations of motion of the i_{th} particle in the vertically two-dimensional coordinate are as follows:

$$\rho\left(\frac{\rho_s}{\rho}+C_M\right)A_3d^3\frac{du_{Pi}}{dt}=\sum_j\left[f_n\cos\alpha_{ij}+f_s\sin\alpha_{ij}\right]_j+\frac{\rho}{2}A_2d^2C_D\left|\mathbf{U}-\mathbf{u}_{pi}\right|\left(U-\mathrm{u}_{Pi}\right) \tag{8}$$

$$\rho\left(\frac{\rho_s}{\rho}+C_M\right)A_3d^3\frac{dv_{Pi}}{dt}=\sum_j\left[-f_n\sin\alpha_{ij}+f_s\cos\alpha_{ij}\right]_j+\frac{\rho}{2}A_2d^2C_D\left|\mathbf{U}-\mathbf{u}_{pi}\right|\left(V-\mathrm{v}_{Pi}\right)-\rho\left(\frac{\rho_s}{\rho}-1\right)A_3d^3g \tag{9}$$

$$\left|\mathbf{U}-\mathbf{u}_{pi}\right|=\sqrt{\left(U-\mathrm{u}_{Pi}\right)^2+\left(V-\mathrm{v}_{Pi}\right)^2} \tag{10}$$

$$\frac{\pi d^4}{32}\frac{d\omega_{Pi}}{dt}=\frac{d}{2}\cdot\sum_j\left(f_s\right)_j \tag{11}$$

in which ρ_s=mass density of sediment particle; C_M=added mass coefficient (=0.5); A_2, A_3= two and three-dimensional geometrical coefficients; d=diameter of particle; u_{pi},v_{pi}=velocity of particles in x and y directions; f_n, f_s=normal and tangential forces acting between i_{th} and j_{th} particles on the n-s local coordinate system (see Fig.1); C_D=drag coefficient (=0.4); α_{ij}=contacting angle between i_{th} and j_{th} particles; $\mathbf{U}$, $\mathbf{u}_{pi}$=velocity vector of fluid and particle, respectively; and ω_{Pi}=rotational angle of the i_{th} particle.

In the case of the uniform-diameter particles, the assessment of contacting particle is simply formulated as

$$\sqrt{\left(x_i-x_j\right)^2+\left(y_i-y_j\right)^2}\le\gamma d \tag{12}$$

in which (x_i, x_j), (y_i, y_j)=coordinates of the centroid of i_{th} and j_{th} particles; and γ=constant around 1.0.

To describe the interparticle collision relation in DEM, between every two contacting particles the spring-dashpot systems should be activated in both normal and tangential directions of the local coordinate, as shown in Fig.1. The acting force

between two adjacent contacting particles i and j can be estimated by

$$f_n(t) = e_n(t) + d_n(t) \tag{13}$$

$$e_n(t) = e_n(t - \Delta t) + k_n \Delta \varsigma_n \tag{14}$$

$$d_n(t) = \eta_n \Delta \varsigma_n / \Delta t \tag{15}$$

$$f_s(t) = e_s(t) + d_s(t) \tag{16}$$

$$e_s(t) = e_s(t - \Delta t) + k_s \Delta \xi_s \tag{17}$$

$$d_s(t) = \eta_s \Delta \xi_s / \Delta t \tag{18}$$

in which e_n, e_s=forces working on springs; d_n, d_s= forces acting on dashpots; $\Delta\zeta_n$, $\Delta\xi_s$=displacement of particles during the time step Δt; k_n, k_s=spring constants; and η_n, η_s=damping coefficients.

Since non-cohesive particle is treated herein, the joint with no resistance to the tensile force is assumed in the normal direction; whereas, in the tangential direction the frictional force activates. Therefore, this characteristic of the joint is featured with the following equations in which joint slips at the limit of the shear stress is applied in the tangential direction:

$$f_n(t) = f_s(t) = 0 \quad when \quad e_n(t) < 0 \tag{19}$$

$$f_n(t) = \mu SIGN[f_s(t), f_s(t)]$$

$$when \quad e_s(t) < \mu e_n(t) \tag{20}$$

$$SIGN[a,b] = \begin{cases} +|a| & when \quad b \geq 0 \\ -|b| & when \quad b < 0 \end{cases} \tag{21}$$

in which μ=friction coefficient (=0.570).

(3) Tuning of the model parameter

According to Cundall and Strack[3], to guarantee the stability of numerical schemes of DEM calculation, the time step Δt should be taken as a fraction of the critical time step or Δt_c. Δt can be estimated on the basis of the Δt_c of the single mass-spring system with a single degree of freedom as

$$\Delta t = \Delta t_c / 20 \quad ; \quad \Delta t_c = 2\pi\sqrt{m / 2k_n} \tag{22}$$

in which m=particle mass.

In this study the time step value is adopted as

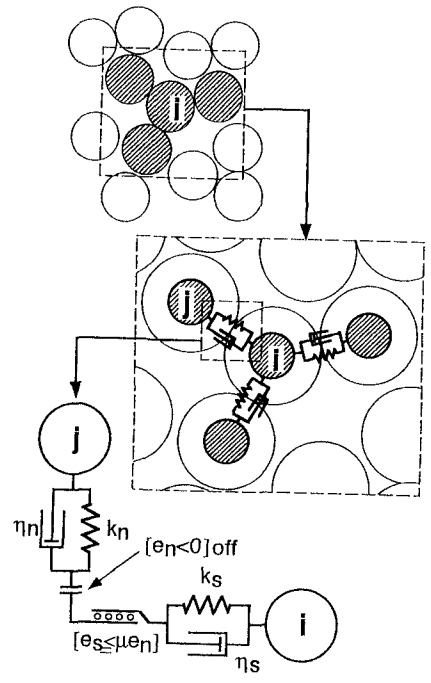

Fig.1 Mulitiparticle collision and interaction system between contacting particles (Gotoh and Sakai[2]).

Δt=0.0002s; thus, k_n is estimated by Eq. 22. From the theory of elasticity k_s is given by

$$k_s = \frac{k_n}{2(1+\nu)} \tag{23}$$

in which ν=Poission's ratio (=0.3).

The damping coefficients are estimated from the following critical damping conditions of Voigt model:

$$\eta_n = \alpha_{cn} 2\sqrt{mk_n} \tag{24}$$

$$\eta_s = \frac{\eta_n}{2(1+\nu)} \tag{25}$$

in which α_{cn}=1.0.

(4) Initial and boundary condition

The vertical coordinate y as well as the calculating domain are schematically shown in Fig.2. Both sides of the calculating domain are periodic to save the calculation time. The boundary condition at the bed is the same as in the steady flow case in which the wall function is implemented, namely the logarithmic law holds between the wall and its adjacent grid point. For the proper fitting of the logarithmic velocity distribution, the theoretical bed level is set below the average height of the particles surface (see Yeganeh[4], for more details). The boundary condition for streamwise velocity at the grid point (y=y_p) in the vicinity of the bottom is the

wall function as follows:

$$\frac{U(y_p,t)}{u_*}=\frac{1}{\kappa}\ln(30.1\frac{y_p}{r_b}) \tag{26}$$

in which κ=von-Kármán constant (=0.41); r_b=bed roughness and u_*=shear velocity.

An additional assumption of the local equilibrium between generation and dissiptaion of turbulent energy is made at the grid point in the vicinity of the bottom wall, hence k and ε at the first grid are calculated by

$$k=\frac{u_*^2}{\sqrt{C_\mu}} \quad ; \quad \varepsilon=\frac{u_*^3}{\kappa y_p} \tag{27}$$

Before the main calculation, the packing calculation was executed to determine the initial location of particles. In the packing procedure, particles are initially arranged with leaving a 0.001cm gap between each other. During the packing process the velocity of particles is monitored to assess the convergence of the packing calculation. After the packing, the main calculation is performed to trace the motion of the sediment under the action of the unsteady fluid flow. The main calculation is consisted of two loops: the outer-loop for the flow calculation and the inner-loop for the MBS calculation. The outer-loop, which equals to one cycle of the oscillatory flow motion, totally takes 4 seconds. In the inner-loop the flow information is feed-backed to the MBS code, and the sediment motion is monitored during the unsteady fluid action. The calculation is continuously performed until it reaches to a fully developed cyclic behavior of sheet flow transport.

The flow depth is 15.0 cm, and the maximum free stream flow velocity is 100.0 cm/s. The test particles are consisted of 0.1, 0.5, 1.0 cm in diameter and 2.65 in specific gravity, respectively. In the calculating domain, totally 50 particles are randomly placed in 10 layers: there are 5 particles in each layer.

3. DISCUSSION AND RESULTS

(1) Mean flow velocity

Figure 3 shows the time series of mean flow velocity distribution, in which the numbers on the figure refer to the phase of the free stream velocity. Near the bottom, it shows the typical feature of oscillatory boundary layer that the velocity close to the boundary is ahead of the free stream velocity in phase. As it might be expected, the thickness of boundary layer varies with the time. On the other hand, the velocity fluctuation estimated by the model is very negligible compare to the periodic velocity component, hence their contribution to the momentum transfer is totally overshadowed by the periodic velocity component, and is not considered in the simulation process (see Sleath[5], for more details.)

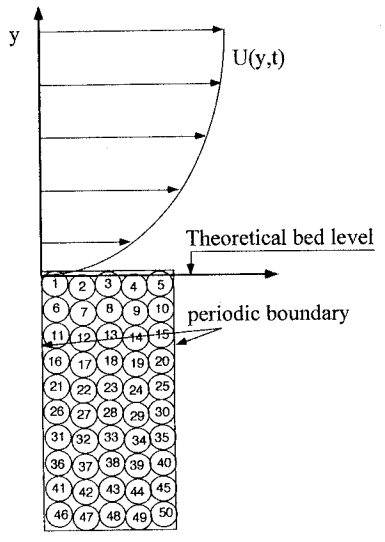

Fig.2 Schematical projection of calculating domain.

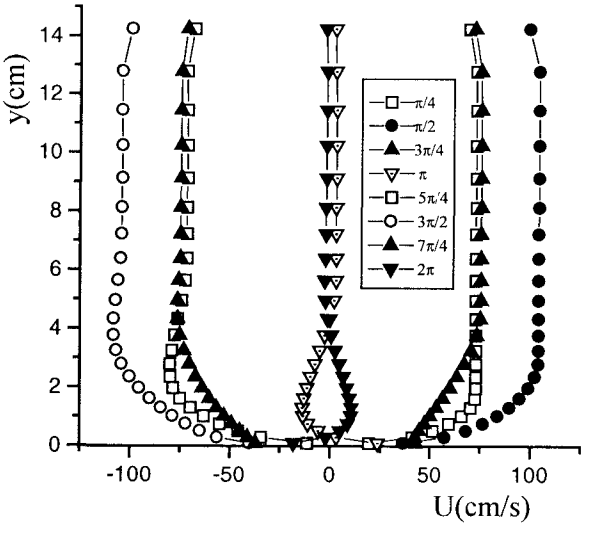

Fig.3 Time series of oscillatory flow velocity.

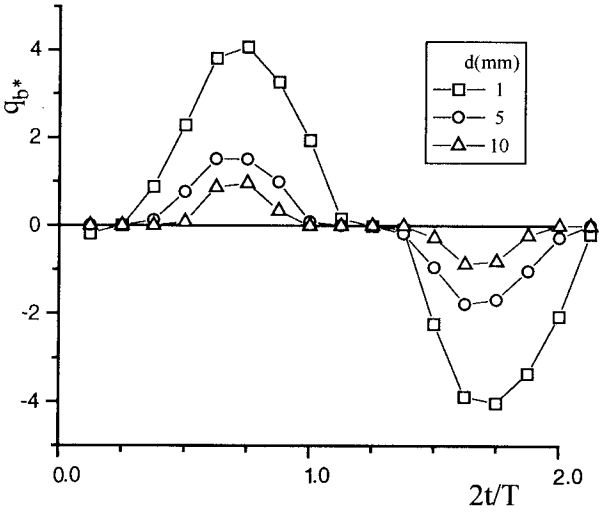

Fig.4 Non-dimensional sheet flow transport rate.

(2) Sheet flow transport rate

Time variation (every $\pi/8$ phase differences) of the non-dimensional sediment transport rate q_{b*}, is depicted in Fig.4. The transport rate is estimated after 10 cycles of calculation time or 40s when the total sheet flow transport rate is almost at a fully developed condition. q_{b*} is defined as follows:

$$q_{b*} = \frac{q_b}{\sqrt{(\rho_s/\rho - 1)gd^3}} \tag{28}$$

in which q_b=sediment transport rate.

The transport rate shows rather simple harmonic behavior and retarded from the free stream flow velocity. The figure indicates that the time variation increases with the particle diameter. For example, in the case of the largest particle (d=1.0cm) this time variation reaches to $3\pi/8$; while, in the case of the smallest one it confines to almost $\pi/4$ or less. On the other hand, the same tendency can not be clearly detected for the maximum transport rate.

As expected, the non-dimensional transport rate shows a clear dependence on the particle diameter, hence the larger particle is, the less rate of transport is induced.

(3) Mean particle velocity

Figure 5 illustrates the streamwise velocity of the particles with the different size at two elevations, namely y/d=0.5 and y/d=-0.5. The streamwise particle velocity is averaged at the final cycle of calculation. The profile of the mean particle velocity has a common trend that the moving particles are retarded from the free stream flow velocity. The same trend is observed in the Fig.4 for the non-dimensional transport rate. However, comparing the Fig.5 with the Fig.4 shows that the time variation in mean particle velocity with the flow frees stream velocity clearly depends on the particle diameter size. The larger the particle is, the time variation is higher.

Moreover, a velocity difference can be observed between the top two layers of the moving sediment in sheet flow layer. This difference is rather negligible in case of the smallest particle (d=0.1cm), whereas for the large particles the differences are considerably large, especially at the phases when the free stream velocity is decelerated.

Therefore, it is evident from Fig.5 that the moving particle does not respond keenly to the flow acceleration and deceleration process in the sheet flow transport layer. Instead the moving particle undergoes rather a moving particle induced process, which is mainly governed by the interparticle collision system. This moving particle induced process is termed herein as the sediment relaxation process. In other words, the motion of particle follows a rather relaxation process that is longer for the larger particles even if they are facing higher rate of flow acceleration and deceleration.

A clear time lag can be seen between the velocity of the free stream flow with the moving particle in the oscillatory sheet flow, which indicates

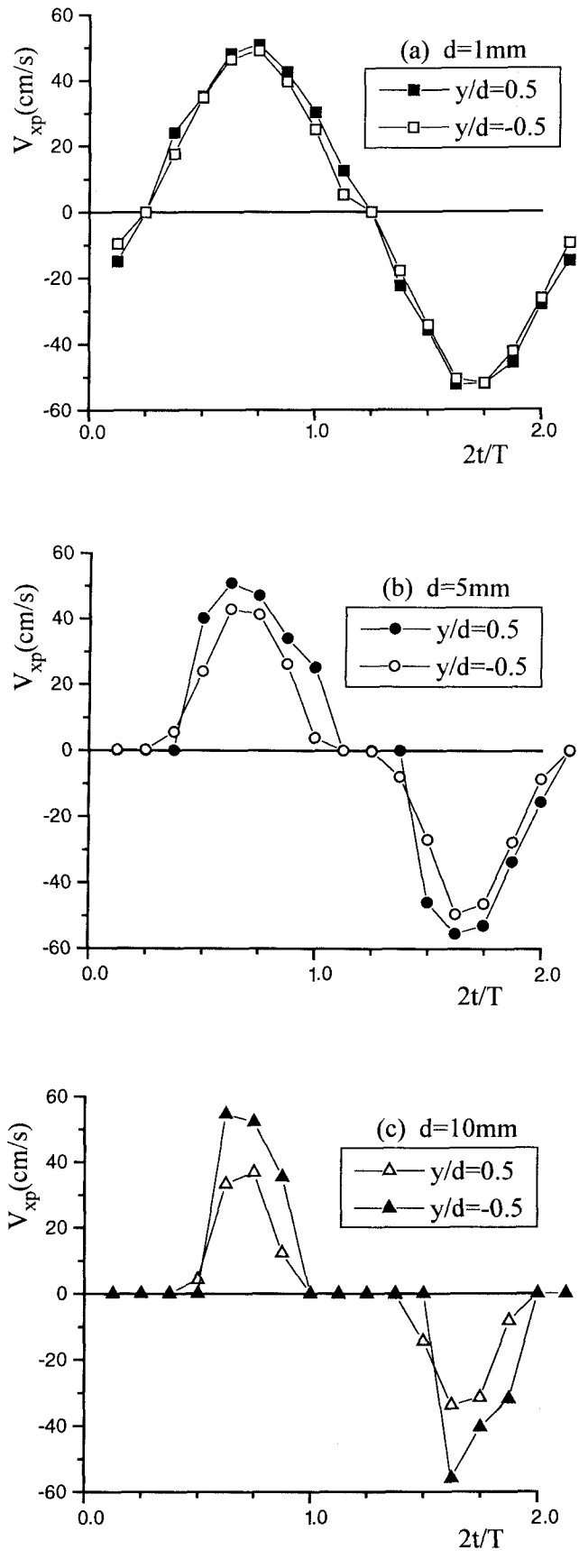

Fig.5 Time dependent particle velocity.

that the larger particle is, the longer the time lag is between the flow and sediment motion. This time lag effect induces skewness in the Figs.4 and 5 for the large particle: the rising limb of the profile shows an upward concave shape, while the falling limb tends to upward convex one. It is evident that under the same flow condition the motion of the large particle takes more time to start, due to inertia effect arising from interparticle collision in sheet flow layer. However, it takes less time for the moving large particles to reach to their maximum velocity in the fluid acceleration and deceleration phases.

(4) Averaged half-cycled transport rate

Fig.6 shows the averaged non-dimensional transport rate under half-sine motion as function of non-dimensional bottom shear stress, τ_*. In connection with oscillatory sheet flow transport, τ_* is generally defined in terms of bottom-shear-stress amplitude, $\tau_{*\max}$ as:

$$\tau_{*\max} = \frac{f U_{\max}^{\ 2}}{2(\rho_s/\rho - 1)gd} \tag{29}$$

in which f=friction factor and $U_{\max}$=maximum free stream velocity. In this study the bed roughness value is adopted as d, and the friction factor for oscillatory flow is estimated based on Tanaka's[6] formula as follows:

$$f = \exp\left[-7.53 + 8.07\left(\frac{U_{\max}}{\omega z_0}\right)^{-0.1}\right] \tag{30}$$

in which ω=radian frequency and z_0=zero-intercept level of logarithmic velocity profile(=d/30).

The transport rate that estimated by the simulation model is found to yield good agreement with the experimental data sets.

4. CONCLUSIVE REMARKS

In this study the development mechanism of oscillatory sheet flow sediment transport and the corresponding particle diameter effect on the transport rate are investigated numerically. The simulation results show that the moving particle in the sheet flow layer does not keenly respond to the flow acceleration and deceleration process. In other words, the moving particles rather induce a complicated relaxation process, which brings a time lag between the flow and the sediment motion. It is concluded, by using three different diameter sizes of sediment, evidently the time lag of the sediment motion in the sheet flow layer depends on the particle diameter size. The larger particle is, the longer time lag is expected.

The profile of the non-dimensional transport rate as well as time dependent velocity of moving particle present a skewness in which the rising limb of the profiles show an upward concave shape, while the falling limb of it tends to upward convex one. Under the same flow condition and intensity

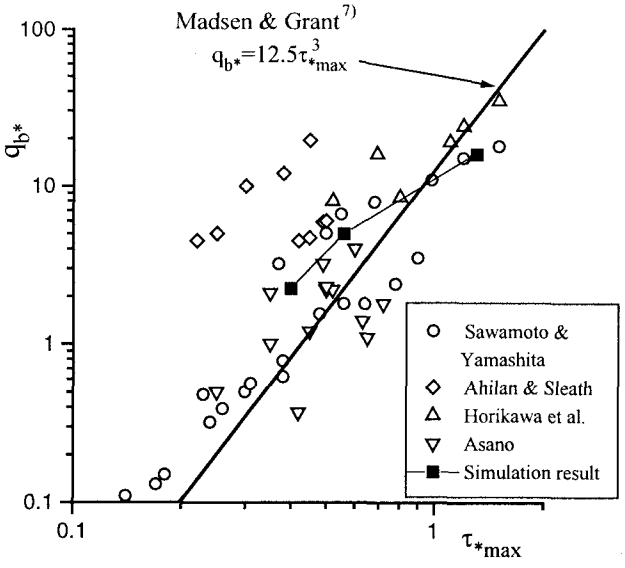

Fig.6 Averaged half-cycled transport rate.

the motion of the large particle in sheet flow layer takes more time to start in the fluid acceleration and deceleration phases, due to inertia effect arises by interparticle collision. However, it takes less time for the moving large particles to reach to their maximum velocity.

ACKNOWLEDGMENT: The authors wish to express their gratitude to Dr. Toshiyuki Asano, Assoc. Prof. of Kagoshima Univ., for his constructive suggestion on the building of the oscillatory flow part of the model, and the Japan Society for Promotion of Science (JSPS) for providing financial support to this research work.

REFERENCES

1) Yeganeh-Bakhtiary, A. and Asano, T.: Effects of particle properties on oscillatory sheet flow dynamics, *Coastal Eng. Jour.* Vol. 40, No. 1, pp. 61-80, 1997.
2) Gotoh, H. and Sakai, T.: Numerical simulation of sheet flow as granular materials, *Jour. of Waterway, Port, Coastal, and Ocean Engrg.*, ASCE, Vol. 123, No. 6, pp. 329-336, 1997.
3) Cundall, P.A. and Strack, O.D.: A discrete numerical model for granular assembles, *Geothechnique 29*, No. 1, pp. 47-65, 1979.
4) Yeganeh-Bakhtiary, A.: Computational mechanics of bed-load transport at high bottom shear, *Doctoral dissertation, Kyoto university*, pp. 94, 1999.
5) Sleath, JFA.: Turbulent oscillatory flow over rough beds, *Jour. Fluid Mech.*, Vol. 182, pp. 369-409, 1987.
6) Tanaka, H. and Tua, A.: Wave-current friction law spanning all flow regimes, *Jour. of Hydraulic, Coastal and Environmental Engrg.*, No. 467/II-23, JSCE, pp. 93-102, 1993. (in Japanese)
7) Madsen, O.S. and Grant, W.D.: Quantitative description of sediment transport by waves. *Proc., 15th Coastal Engrg., Conf.*, ASCE, New York, pp. 1093-1112, 1976.

(Received September 30, 1999)